

METHODS ARTICLE

In vitro fluorescence assay to measure GDP/GTP exchange of guanine nucleotide exchange factors of Rho family GTPases

Alyssa M. Blaise ^{1,2}, Ellen E. Corcoran^{1,2}, Eve S. Wattenberg^{1,2}, Yan-Ling Zhang³, Jeffrey R. Cottrell³ and Anthony J. Koleske^{1,2,*}

¹Departments of Molecular Biophysics and Biochemistry, Yale School of Medicine, Yale University, New Haven, CT 06520-8024, USA, ²Neuroscience, Yale School of Medicine, Yale University, New Haven, CT 06520-8024, USA and ³Stanley Center for Psychiatric Research, Broad Institute of MIT and Harvard, Cambridge, MA 02142, USA

*Correspondence address. Departments of Molecular Biophysics and Biochemistry, Yale School of Medicine, Yale University, New Haven, CT 06520-8024, USA. Tel: 203-785-5624; E-mail: anthony.koleske@yale.edu

Abstract

Guanine nucleotide exchange factors (GEFs) are enzymes that promote the activation of GTPases through GTP loading. Whole exome sequencing has identified rare variants in GEFs that are associated with disease, demonstrating that GEFs play critical roles in human development. However, the consequences of these rare variants can only be understood through measuring their effects on cellular activity. Here, we provide a detailed, user-friendly protocol for purification and fluorescence-based analysis of the two GEF domains within the protein, Trio. This analysis offers a straight-forward, quantitative tool to test the activity of GEF domains on their respective GTPases, as well as utilize high-throughput screening to identify regulators and inhibitors. This protocol can be adapted for characterization of other Rho family GEFs. Such analyses are crucial for the complete understanding of the roles of GEF genetic variants in human development and disease.

Keywords: guanine nucleotide exchange factor (GEF); Rho family GTPase; Trio protein

Introduction

Rho family GTPases are master regulators of the actin cytoskeleton [1–3]. They act as binary molecular switches, cycling between an inactive GDP-bound state and an active GTP-bound state. In their active state, distinct Rho family GTPases engage multiple specific effectors to coordinate dynamic rearrangements of the actin cytoskeleton. Such rearrangements have been best characterized for the GTPases RhoA, Rac1, and Cdc42. RhoA:GTP activates downstream kinase target Rho Kinase (ROCK) [4], upon activation, ROCK phosphorylates

myosin light chain to promote actomyosin contractility in cells [4, 5]. Rac1:GTP and Cdc42:GTP stimulate Wiskott–Aldrich Syndrome family proteins which are used to activate new actin filament nucleation through the Arp2/3 complex and promote actin-based cell edge protrusions [6–9]. In this manner, Rho family GTPases direct dynamic changes in actin polymerization, actin filament severing, actin filament coupling to the membrane and actomyosin contractility. These cytoskeletal rearrangements promote changes in cell shape and movement in a wide variety of cellular contexts, including cell migration,

Received: 13 September 2021; **Revised:** 14 December 2021; **Editorial Decision:** 15 December 2021

© The Author(s) 2021. Published by Oxford University Press.

This is an Open Access article distributed under the terms of the Creative Commons Attribution-NonCommercial License (<https://creativecommons.org/licenses/by-nc/4.0/>), which permits non-commercial re-use, distribution, and reproduction in any medium, provided the original work is properly cited. For commercial re-use, please contact journals.permissions@oup.com

phagocytosis, endocytosis, morphogenesis and cytokinesis [10, 11].

The cycling of Rho-GTPases between their GDP- and GTP-bound states is regulated by two classes of proteins: GTPase activating proteins (GAPs) and Guanine nucleotide exchange factors (GEFs). GAPs act as Rho-GTPase inhibitors by promoting hydrolysis of bound GTP. In contrast, GEFs promote the dissociation of GDP from the inactive Rho:GDP complex. This dissociation enables GTP, which is present at significantly higher cellular concentrations than GDP, to bind to and activate the GTPase (Figure 1) [12]. Rho-GEF domains contain two parts: a Dbl-homology (DH) domain and a regulatory pleckstrin homology (PH) domain. The DH domain catalyzes nucleotide exchange [13–16]. The PH domain regulates GEF activity by binding phospholipids that tether GEFs to the cellular membrane [17]. This binding either allosterically inhibits the GEF domain [18, 19] or facilitates catalysis via direct interactions with the Rho family GTPase substrate [20–23]. These multiple modes of regulation enable GEFs to serve as central signaling hubs that tightly coordinate signals between cell-surface receptors and downstream cytoskeletal arrangements.

Due to these multiple modes of regulation, it is not surprising that Rho-GTPases play integral roles in neuronal development and function via their regulation of actin dynamics [24]. Of the 71 DH–PH domain-containing GEFs in the human genome, over half of them are expressed in the developing brain [25–28]. Rho-GEFs play diverse roles in coordinating neuronal migration, differentiation, axon and dendrite formation, and synaptogenesis [29–31]. Advances in whole-exome and whole-genome sequencing technologies have enabled the field to find mutations and rare coding variants associated with neurodevelopmental disorders. Unsurprisingly, mutations and rare variants in Rho-GEFs are associated with several neurodevelopmental disorders [32–37].

Recent findings have provided insights into the mechanisms involved in Rho-GEF-mediated neuronal development and how these mechanisms are disrupted in disease. For example, de novo mutations and ultrarare disease-associated variants have been found in the *TRIO* gene [34, 37–42]. *TRIO* encodes a large protein

with three catalytic domains: two DH–PH Rho-GEF domains and a putative serine threonine kinase domain (Figure 2) [43]. The first DH–PH module, the GEF1 domain, can activate Rac1 and RhoG GTPases, while the second module, the GEF2 domain, activates RhoA. Many of the disease-related mutations and rare variants lie within or adjacent to the GEF1 and GEF2 domains.

Systematically measuring the impact of each of these mutations on activity is critical, as mutations that alter Trio GEF1 activity are associated with distinct clinical outcomes [44]. Previous studies have used protein pull-down assays to assess Rho [45] and Rac1 GTPase activity [46]. While this method permits the measurement of the relative activation of the GTPase, it does not measure the relative catalytic rate or efficiency of a Rho-GEF. Fluorescence assays that monitored GDP/GTP exchange on various GTPases were developed as a more robust and reproducible quantitative assay for GEF activity. The first of such *in vitro* fluorescence assays typically used mant-GDP, a fluorescent GDP analog. mant-GDP exhibits increased fluorescence upon binding to Rho GTPases. Rho-GEF-mediated exchange of mant-GDP for GTP led to a reduction in fluorescence over time [47, 48]. Improvements came in the use of BODIPY-FL-guanine nucleotides which exhibit increased signal to noise. The binding or dissociation of BODIPY-FL-guanine nucleotides from GTPases could be measured by either change in fluorescence [49, 50] or change in polarization of the fluorescent nucleotide [51, 52].

Here, we provide a detailed, user-friendly protocol for measuring the specificity and efficiency of the guanine nucleotide exchange activities of TRIO, which has two GEF domains with distinct catalytic activities (Figure 3). We first describe the procedure for expression and purification of Trio GEF1/GEF2 and Rho GTPases Rac1, RhoA, and Cdc42. We then describe the use of a fluorescence-based assay to measure the guanine nucleotide exchange activity for both Trio GEF domains. This assay monitors Trio GEF activity by measuring the decrease in fluorescence intensity as fluorescent BODIPY-GDP bound to the Rho-GTPase (Rac1 or RhoA) is exchanged for non-fluorescent GTP. We have also developed software to enable facile data

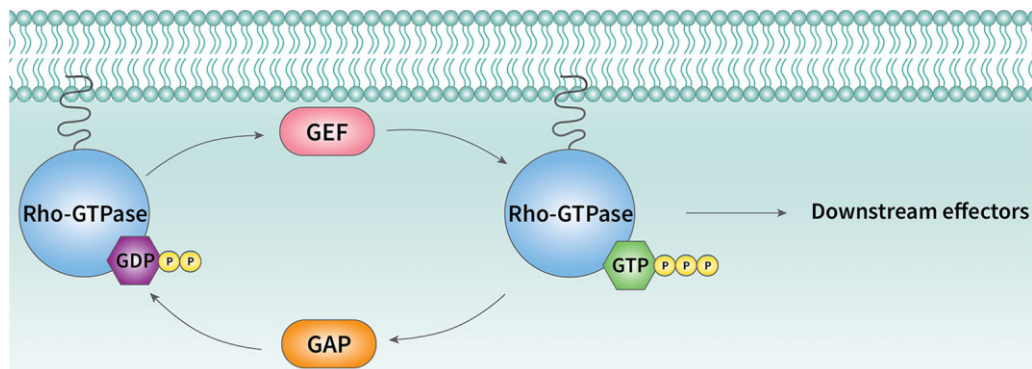


Figure 1: GDP/GTP cycling of Rho family GTPases. Rho family GTPases remain in their inactive state when they are GDP-bound. They are activated by GEFs which catalyze the exchange of GDP for GTP. Once GTP is bound, Rho family GTPases are in their active state and signal to downstream effectors that regulate the actin cytoskeleton.

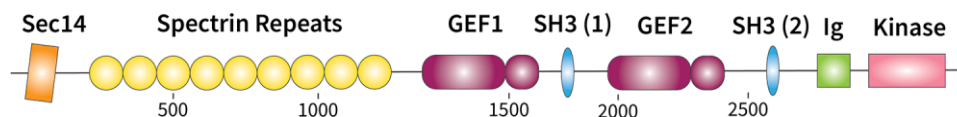


Figure 2: Trio protein structure. Trio has multiple catalytic domains. The Sec14 domain, the SH3 domains, and spectrin repeats mediate lipid protein and cytoskeleton interactions. The kinase domain phosphorylates serine and threonine. The two GEF domains regulate the exchange of GDP for GTP on small Rho family GTPases, Rac1/RhoG, and RhoA.

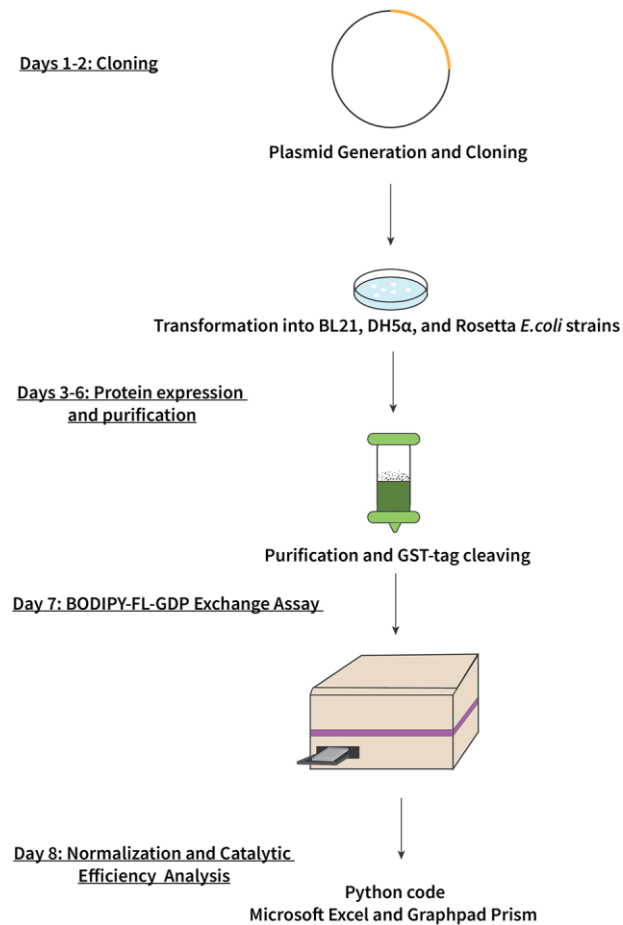


Figure 3: Graphical summary of methods. Rho family GTPase and Trio GEF plasmids were generated and cloned on days 1 and 2. Recombinant protein was expressed and purified on days 3 and 6. A BODIPY-FL-GDP fluorescence-based exchange assay was performed on day 7 to assess Trio GEF activity. Data were processed using Python code and catalytic efficiency was determined.

processing to calculate catalytic rate and efficiency. Finally, we demonstrate that this assay is scalable for a high-throughput setting for potential use in identifying small-molecule regulators of GEFs. This assay allows for a quantitative analysis of GEF activity on many Rho-GTPases that can advance understanding of the impacts GEFs have on human disease.

Materials and methods

Generation of DNA expression constructs

pGEX6P1-based plasmids encoding GST-tagged GTPases (GST-RhoA, GST-Rac1, and GST-Cdc42) were PCR amplified from cDNAs encoding mouse/human RhoA, Rac1, and Cdc42 utilizing the following primers:

Rac1 primers

Sense: 5'-GATCGGATCCATGCAGGCCATCAAGTGTGTG-3'
Antisense: 5'-GATCGCGGCCGCTTAGAGGACTGCTCGGATCGC-3'

The amplified PCR product of 548 nucleotides encodes the amino acids Glu 2 to Leu 179 of Rac1 flanked by the shaded BamHI (5'-GGATCC) and shaded NotI site (CGCGCCGC-3') fuses Rac1 in frame to glutathione S-transferase.

RhoA primers

Sense: 5'-GATCGGATCCATGGCTGCCATCCGGAAGAAA-3'
Antisense: 5'-GATCGCGGCCGCTCACAAGACAAGGCACCCAGA-3'

The amplified PCR product of 596 nucleotides encodes the amino acids Ala 2 to Leu 193 of RhoA flanked by the shaded BamHI (5'-GGATCC) and shaded NotI site (CGCGCCGC-3') fuses RhoA in frame to glutathione S-transferase.

Cdc42 primers

Sense: 5'-GATCGGATCCATGCAGACAATTAAGTGTGTTA-3'
Antisense: 5'-GATCGCGGCCGCTCATAGCAGCACACACTGGC-3'

The amplified PCR product of 590 nucleotides encodes the amino acids Glu 2 to Leu 191 of Cdc42 flanked by the shaded BamHI (5'-GGATCC) and shaded NotI site (CGCGCCGC-3') fuses Cdc42 in frame to glutathione S-transferase.

These PCR products were digested with the indicated restriction enzymes and inserted into the cognate sites of pGEX6P1. All constructs were verified by DNA sequencing.

pET-His-TT-based plasmids encoding His-tagged GEF1 and GEF2 were constructed following PCR amplification from cDNAs encoding human Trio using the following primers:

TRIO GEF1 primers

Sense: 5'-GATCGGATCCATGGGCTCAGAGGTGAAACTT-3'
Antisense: 5'-GATCGCGGCCGCTACTTAGGGATGTGAATGGG-3'

This set of primers amplified a PCR fragment of 1026 nucleotides, which was cloned into the shaded BamHI (5'-GGATCC) and shaded NotI (CGCGCCGC-3') sites of pET-His-TT. The amplified product encodes the Trio GEF1 domain from amino acid Gly 1270 to Pro 1608.

TRIO GEF2 primers

Sense: 5'-GATCGGTACCATGGAAGAAAGAAATCCAGCA-3'
Antisense: 5'-GATCGCGGCCGCCCTACCCGCTGTGGTTCCTC-3'

This set of primers amplified a PCR fragment of 1005 nucleotides, which was cloned into the shaded KpnI (5'-GGATCC) and shaded NotI (CGCGCCGC-3') sites of pET-His-TT. The amplified product encodes the Trio GEF2 domain from amino acid Glu 1960 to Gln 2287.

Protein expression and purification

In pilot testing, we transformed each expression plasmid separately into BL21, DH5 α , and Rosetta *Escherichia coli* strains to optimize expression and solubility of the respective protein.

Purification of GST-RhoA and GST-Rac1

Day 0: Plasmids were transformed fresh into BL21 cells and plated onto agar plates containing 100 μ g/mL ampicillin. The plates were incubated at 37°C overnight.

Day 1: A single BL21 colony was used to inoculate 50 mL of 2XYT media (16 g/L tryptone, 10 g/L yeast, 5.0 g/L NaCl, pH = 7.0) containing 200 μ g/mL ampicillin to maintain high plasmid copy number and 0.2% glucose to prevent possible slow growth due to expression of the recombinant protein. Starter cultures were grown for ~12–18 h at 37°C on a shaking platform at 200 rpm. Sixteen milliliters (each) of the starter culture was used to inoculate 4 \times 800 mL cultures in 2XYT containing 200 μ g/mL ampicillin. The initial culture density was measured (typically OD₆₀₀ \approx 0.050). These cultures were incubated on a shaking platform at 37°C to an OD₆₀₀ = 0.6–0.8, then shifted to 16°C to equilibrate. After approximately 60 min, when OD₆₀₀ = 0.8–1.0,

expression of the GTPase proteins was induced by adding IPTG to 0.5 mM and incubating the culture on a shaking platform at 200 rpm in 16°C overnight. We have found that overnight induction at 16°C of the Trio GEF1 domain, Trio GEF2 domain, and Rho family GTPases reduces protein degradation. Overnight induction at 16°C also provides the optimal timing for bacterial cell mass to grow, allowing the investigator to begin protein purification first thing in the morning.

Day 2: Bacteria were pelleted via centrifugation for 20 min at 15 000 rpm in an SA-600 centrifuge. Cell pellets were resuspended in a total volume of 48 mL of ice-cold lysis buffer containing 1× PBS (8 mM Na₂HPO₄·7H₂O, 2 mM KH₂PO₄, 137 mM NaCl, 2.7 mM KCl), 5% glycerol, 1 mM EDTA, 1 mM DTT, 1 mM PMSF, and protease inhibitors (in all cases, we use 1× Sigma Aldrich cOmplete protease inhibitor cocktail). If needed, the resuspended cell pellets can be frozen in 50 mL Falcon tubes using liquid nitrogen and stored at –80°C for later purification. We have stored material in this manner for up to 2 weeks with no loss in the quality of the purified material.

Resuspended cell pellets were thawed in a water bath and quickly put on ice. The pellets were subject to sonication at maximal output on a 50% duty cycle for 4 × 3 min, pausing in between cycles to swirl the lysates on ice and cool the sample. Following sonication, Triton X-100 was added to 1% to the lysate and gently mixed. This mixture was allowed to incubate for 20 min on ice. The lysate was loaded into Oak Ridge tubes and centrifuged at 4°C in an SA600 Rotor for 30 min at 15 000 rpm. The supernatant was loaded into a 50-mL syringe and filtered through a 0.45-μm syringe top filter. Two milliliters of glutathione-agarose bead slurry (Pierce) was washed 3× in ice-cold 1× PBS (1.5 mM KH₂PO₄, 155 mM NaCl, 2.7 mM Na₂HPO₄·7H₂O). The beads were packed into a 10-mL disposable chromatography column (Pierce Protein Solutions, ThermoFisher). The lysate supernatant was run through the column 3× and washed three times with 10 mL of 1× PBS, 5% glycerol, 1 mM DTT, and 1 mM PMSF, and equilibrated with 10 mL of equilibration buffer (20 mM HEPES pH = 7.25, 150 mM KCl, 5% glycerol, 1 mM DTT, 0.01% Triton X-100, and 1 mM PMSF). Fractions were eluted in 1 mL aliquots of elution buffer (20 mM HEPES pH = 7.25, 150 mM KCl, 5% glycerol, 1 mM DTT, 0.01% Triton X-100, 10 mM glutathione, buffered to pH = 7.25). Protein elution was monitored using a Bradford assay. Eluted protein fractions were pooled and incubated with PreScission Protease (5 units/mg) overnight to cleave off the GST-tag. The following day, the protein mixture was concentrated by centrifugal filtration and GST was separated from the GTPase by size exclusion chromatography into GTPase exchange buffer (20 mM HEPES pH = 7.25, 150 mM KCl, 5% glycerol, 1 mM DTT, and 0.01% Triton X-100) on a Superdex 75 column (GE). A series of 2-fold dilutions of a bovine serum albumin (BSA) protein standard in Bradford reagent ranging from 0 to 2 mg/mL were prepared to create a standard curve used for calculating protein concentration. Two microliters of each BSA dilution was added to 200 μL of diluted Bradford reagent. Often, the eluted protein was too concentrated to be in the linear range of detection when added to Bradford reagent. The purified protein sample was diluted in elution buffer, 1:5, 1:10, and 1:20, depending on the concentration of protein eluted. Two microliters of each protein dilution was added to 200 μL of Bradford reagent. Absorbance levels of both the BSA and protein dilutions were measured at 595 nm on a spectrophotometer. The standard curve was created for the BSA dilutions using absorbance (A₅₉₅) versus concentration. The unknown concentration of the purified protein was determined from an absorbance (A₅₉₅) versus BSA concentration plot. Protein purity was

evaluated after running 10 μg of protein using SDS-Page and Coomassie blue staining with analysis in Image J. GTPase was aliquoted for assay use and stored at –80°C.

Purification of TRIO His-GEF domains

Days 0–1 were followed as described above using plasmids encoding His-tagged TRIO GEF domains, His-GEF1 and His-GEF2.

Day 2: Bacteria were pelleted via centrifugation for 20 min at 4000 rpm in an RC3B centrifuge and cell pellets were resuspended in a total volume of 48 mL of ice-cold His lysis buffer (20 mM Hepes pH = 7.25, 500 mM KCl, 5% glycerol, 1% Triton X-100, 20 mM imidazole pH 7.25, 5 mM β-mercaptoethanol, 1 mM DTT, 1 mM PMSF, and protease inhibitors). The resuspended cells were sonicated as described above and centrifuged at 4°C in an SA600 Rotor for 30 min at 15,000 rpm. The supernatant was loaded into a 50-mL syringe and filtered through a 0.45-μm syringe top filter. One milliliter of Ni-NTA agarose bead slurry (Thermo Fisher) was washed 3× with ice-cold buffer (20 mM Hepes pH = 7.25, 150 mM KCl, 5% glycerol, 1% Triton X-100, 20 mM imidazole pH 7.25, 5 mM β-mercaptoethanol, 1 mM DTT, 1 mM PMSF, and protease inhibitors) and packed into a 10 mL disposable chromatography column (Pierce Protein Solutions, Thermo Fisher). The clarified lysate was passed through the column 3× and washed with 10 mL of wash buffer A (20 mM Hepes pH = 7.25, 150 mM KCl, 5% glycerol, 0.1% Triton X-100, 20 mM imidazole pH 7.25, 5 mM β-mercaptoethanol, 1 mM DTT, and 1 mM PMSF), 10 mL of wash buffer B (20 mM Hepes pH = 7.25, 150 mM KCl, 5% glycerol, 0.01% Triton X-100, 5 mM MgCl₂, 10 mM ATP, 1 mM DTT, 1 mM PMSF, adjusting pH to 7.25 with KOH, if needed), and 10 mL of wash buffer C (20 mM Hepes pH = 7.25, 150 mM KCl, 5% glycerol, 0.01% Triton X-100, 1 mM DTT, and 1 mM PMSF). Bound protein was eluted in 0.5 mL aliquots of His elution buffer (20 mM Hepes pH = 7.25, 150 mM KCl, 5% glycerol, 0.01% Triton X-100, 1 mM DTT, 250 mM imidazole pH 7.25, 1 mM PMSF, and protease inhibitors). The protein concentration and purity were determined as stated above. We typically do not cleave the His-tag, as cleaving it from the Trio GEF1 and GEF2 domains does not impact GEF catalytic activity. Purified protein fractions were dialyzed for 4–6 h using 2 L of dialysis buffer (20 mM Hepes pH = 7.25, 150 mM KCl, 5% glycerol, 1 mM DTT, 0.01% Triton X-100, and 1 mM PMSF) then overnight in 2 L of fresh dialysis buffer. The Trio GEF domains were aliquoted, flash frozen in liquid nitrogen, and stored at –80°C for later use.

BODIPY-FL-GDP nucleotide exchange assays

Prior to assay use, all protein aliquots were thawed on ice and centrifuged for 10 min at 15,000 rpm to remove any debris. Protein concentration was measured again via Bradford (as described above) to verify protein concentration. 12.8 μM Rac1, RhoA, or Cdc42 (data not shown) was loaded with 3.2 μM BODIPY-FL-GDP in 1× exchange buffer (20 mM Hepes pH = 7.25, 150 mM KCl, 5% glycerol, 1 mM DTT, and 0.01% Triton X-100) plus 2 mM EDTA to a total volume of 25 μL per reaction, then incubated for 1 h at room temperature. The reaction was protected from light with aluminum foil. GTPases were loaded at a ratio of 1:4 BODIPY-FL-GDP to GTPase, respectively, to minimize background fluorescence. Loading of BODIPY-FL-GDP was halted by the addition of 5 μL of MgCl₂ to block further GDP binding to GTPase, for a total volume of 30 μL with a final MgCl₂ concentration of 30 mM. Prior to initiating the reaction with Trio GEF, 30 μL of GTPase (12.8 μM) plus MgCl₂ (30 mM) or blank (3.2 μM BODIPY-FL-GDP, 2 mM EDTA, 1× exchange buffer) was

added to appropriate wells, followed by shaking of the plate for 30 s and 10 min of room temperature incubation. During this incubation period, various Trio GEF1/GEF2 concentrations were prepared in 1× Buffer (20 mM Hepes pH = 7.25, 150 mM KCl, 5% glycerol, 1 mM DTT, and 0.01% Triton X-100), 4 mM GTP, and 2 mM MgCl₂. GEF mixes were mixed well and placed on ice until use. Exchange reactions were started by adding 10 μL of respective Trio GEF concentration mixture (as stated above) to each well, for a total reaction volume of 40 μL. Reactions were mixed carefully to avoid bubbles. After shaking the plate again for 30 s, real-time fluorescence data were measured every 10 s for 30 min monitoring BODIPY-FL fluorescence by excitation at 488 nm and emission at 535 nm. For these measurements, we set the photomultiplier tube (PMT) gain to 325 V, but note that this setting may need to be adjusted depending on the sensitivity of the instrument.

Data processing and analysis of catalytic rate and efficiency

Data from the assay were processed using a custom script in Anaconda distribution of Python (see [Supplementary Materials](#)). The script is a text-based program that runs from a command line. The code takes in raw time-series plate reader data as a .xls spreadsheet. The user must convert the .xls to .xlsx prior to processing the data via the script. The user specifies which wells were used for background and which wells contained each experimental condition. Data from wells that were not part of the experiment are discarded. Wells for which some or all observations fell below the background value are automatically flagged as possibly containing a bubble. The program then calculates the average time series for each experimental condition and subtracts the background value. The user can opt to normalize the data so that the first observation for each averaged time series has a value of 1. Raw or normalized fluorescence averages are then visualized in a time-series line plot that may be saved in a .png format. The relabeled data may be saved for further analysis as either a .csv or .xlsx file, with or without the averages and normalizations. We have run the program successfully on macOS High Sierra using the built-in Terminal and Windows 10 using Anaconda Prompt, processing data from a Molecular Devices SpectraMax M5 plate reader. Data saved as .csv can be imported to GraphPad Prism 8. Because the fluorescence of GDP-FL-BODIPY decreases exponentially over time, the fluorescence curves can be fit to a one-phase exponential decay function to determine the catalytic rate (λ) of Trio GEF activity using Equations (1)–(3):

$$Y_t = Y_0 e^{-t/\tau}, \quad (1)$$

$$\lambda = \frac{1}{\tau}, \quad (2)$$

$$t_{1/2} = \frac{\ln(2)}{\lambda} = \tau * \ln(2), \quad (3)$$

where Y_t is the fluorescence intensity at time t and Y_0 is the initial intensity at time $t=0$. τ is the time constant, expressed in the same units as the X-axis. It is computed as the reciprocal of the catalytic rate, λ . The half-life, $t_{1/2}$, is the time required for the amplitude to be one half of its initial value. A pseudo first-order rate constant (observed rate constant or K_{obs}) can be calculated from the data because the reaction contains a large excess of GTP over GTPase.

GraphPad Prism 8 can be used to execute this fit. After opening GraphPad Prism 8 and creating a new XY table, the time can be entered into X and fluorescence readings into Y. The X units can be marked “Seconds” for analysis by selecting “Format Data Table” from the Change Menu. After entering data (X units), the “Analyze” button can be selected, followed by “Nonlinear Regression” from the list of XY analyses. “One phase exponential decay” can be selected to obtain the first-order K_{obs} value, or λ (s^{-1}). Because the derivative of an exponential decay equals $-\lambda * Y$, the initial rate can be calculated as $-\lambda * Y_0$. When testing multiple GEF concentrations, the catalytic efficiency (K_{cat}/K_M) can be extracted from a plot of catalytic rate (s^{-1}) versus GEF concentration that is fit with a linear function using Microsoft Excel.

High-throughput guanine nucleotide exchange assay and screening

For high-throughput screening, the Trio GEF1 or GEF2-mediated rate of nucleotide exchange was monitored using a Fluorescence Imaging Plate Reader (FLIPR). Compound was first incubated with GEF1 for 10 min in 384-well clear bottom Corning microplates. The nucleotide exchange process was initiated by adding Rac1, pre-loaded with BODIPY-FL-GDP, through an in-line liquid dispenser building within FLIPR ([Figure 6](#)). Reactions containing GEF1 and GTP were initiated by in-line liquid transfer of 1.5 μM RhoA pre-loaded with BODIPY-FL-GDP. The kinetic reaction for the exchange assay was measured continuously from the well-bottom using fluorescence imaging for 10 min. The initial fluorescence change (slope of fluorescence) from dissociation of BODIPY-GDP from the Rac1-bound form indicated a linear relationship with concentration of GEF1 and BODIPY-GDP-bound Rac1. In total, 2 μM BODIPY-GDP loaded Rac1 and 0.2 μM GEF1 was used for high-throughput screening since these conditions allowed for the detection of both inhibition and activation of GEF1-catalyzed nucleotide exchange. This allowed for the potential identification of both activators and inhibitors of GEF activity.

Results

GST-tagged proteins were purified with an average yield of ~20 mg with 94% purity for Rac1 and 99% purity for RhoA ([Figure 4](#)). His-tagged proteins were purified with an average yield of ~30 mg with 95% purity for GEF1 and 94% purity for GEF2 purity ([Figure 4](#)). Purified proteins were utilized in our

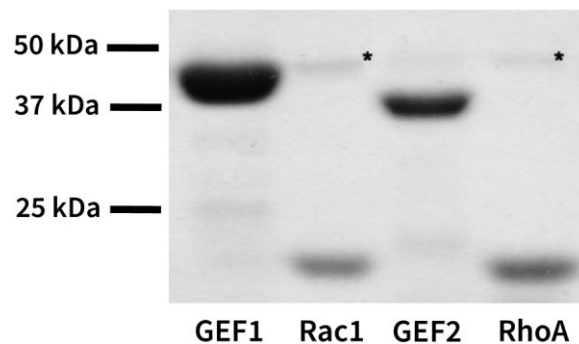


Figure 4: Purified proteins used in GEF assays. Coomassie Blue staining of the purified proteins Trio GEF1, Rac1, Trio GEF2, and RhoA following overexpression in bacteria. The % purity of each protein calculated using Image J is as follows: Trio GEF1 95%, Trio GEF2 94%, Rac1 94%, and RhoA 99%. Asterisks indicate preScission protease residue used to cleave GST-tags off protein that do not impact the assay.

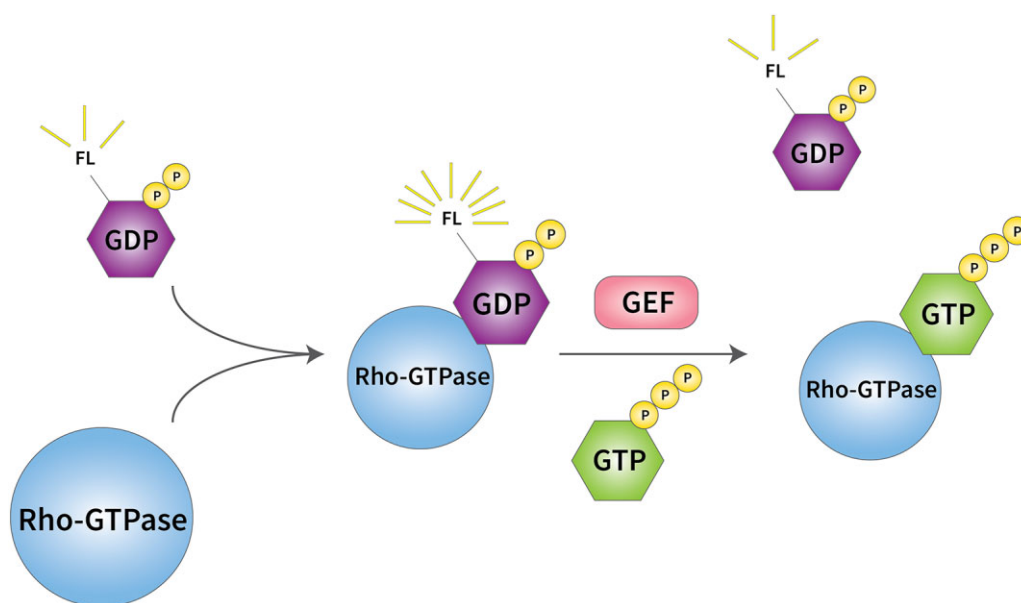


Figure 5: GEF activity assay. This assay measures the ability of the GEF domains to catalyze the exchange of GDP for GTP on their respective small, Rho family GTPases. Free fluorescent BODIPY-FL-GDP has a low fluorescence. Fluorescence increases when BODIPY-FL-GDP binds to Rac1. GTP is introduced and GEF catalyzes the exchange of BODIPY-FL-GDP for GTP on Rac1 causing a decrease in fluorescence.

BODIPY-FL-GDP exchange assay with the goal of determining Trio GEF1/2 specificity for the Rho GTPases Rac1 and RhoA. BODIPY-FL-GDP emits little fluorescence in solution, but this increases 4-5-fold upon binding GTPases (Figure 5). In the presence of GTP and Mg^{2+} , Trio GEFs catalyze the exchange of BODIPY-FL-GDP for GTP on Rho family GTPases, leading to an exponential decrease in BODIPY-FL-GDP fluorescence in a time- and GEF concentration-dependent manner. Each experimental group was performed in triplicate. Negative controls for this experiment include a reaction containing BODIPY-FL-GDP with no GTPase and a reaction containing GTPase loaded with BODIPY-FL-GDP, but no GEF. Trio GEF1 catalyzed efficient nucleotide exchange on Rac1 (Figure 6A) with a catalytic rate of $k_{obs(250\text{ nM GEF1})} = 0.00532\text{ s}^{-1}$ and a catalytic efficiency of $k_{cat}/K_m = 2.14 \times 10^4\text{ M}^{-1}\text{ s}^{-1}$ (Figure 6C). Trio GEF2 was similarly efficient in catalyzing nucleotide exchange on RhoA (Figure 6B) with a $k_{obs(250\text{ nM GEF2})} = 0.00598\text{ s}^{-1}$ and a $k_{cat}/K_m = 2.39 \times 10^4\text{ M}^{-1}\text{ s}^{-1}$ (Figure 6D). GEF1- and GEF2-mediated exchange was specific: Trio GEF1 did not catalyze significant nucleotide exchange on RhoA (Figure 6E, G) and Trio GEF2 did not exhibit significant exchange on Rac1 (Figure 6F, H).

This assay can be readily scaled up to a 384-well assay for high-throughput screening (Figure 6I). A CNS-focused library of 5100 small molecules was screened in duplicate as a pilot to validate the novel screening assay and identify potential regulators that modulate the rate of GEF1 or GEF2-catalyzed nucleotide exchange of Rac1 or RhoA. Initial fluorescence change rate for each well was captured and analyzed in Genedata (RRID: SCR_021326). This assay achieved a 10-fold signal to background window and an average Z' factor of 0.6 (using no GEF1 as inhibitor control), indicating it is an excellent assay for primary high-throughput screening. The hit compounds from the pilot screening were selected using a cut-off of three standard deviations from the mean of the total measured compounds. Twenty inhibitor hits were identified in a pilot screen for a 0.4% hit rate (Figure 7A) and 16 activator hit compounds were identified (Figure 7B) for a 0.3% hit rate. A dose-response experiment starting from $100\text{ }\mu\text{M}$ of each compound with 2-fold sequential

dilutions was carried out for confirmation of hits, but unfortunately none showed significant potency upon dilution ($IC_{50} > 100\text{ }\mu\text{M}$ for all compounds). It is possible that increasing the chemical space beyond 5100 compounds probed would yield more promising hits. We validated this assay by testing several published Trio GEF1 regulators including NSC23766 [53, 54], ITX3 [55], CPYPP [56], $EH_{op}016$ [57], and EHT1864 [58], however, none of them reached our potency threshold (Figure 7C). For example, the Trio GEF1 inhibitor ITX3 showed ~40% inhibition against GEF1 at $250\text{ }\mu\text{M}$, which is less potent than previously published data ($IC_{50} \sim 76\text{ }\mu\text{M}$) when RhoG was used as a substrate [55] (Figure 7D). It is possible that there is a potency difference when Rac1 is used as a substrate when compared with RhoG.

Discussion

We described an assay developed to demonstrate the specificity of Trio GEFs for the various Rho family GTPases. Similar approaches are directly applicable to GEFs for other GTPases. This assay enables a quantitative analysis of catalytic efficiency of the GEFs and can also be scaled up for a high-throughput screening for small molecule GEF regulators.

It is especially important to properly understand how Trio GEF activity changes with several disease-related mutations [37, 59]. Since these mutations are directly related to clinical outcomes, understanding the change in this activity could prove beneficial for developing small molecule modulators of GEF activity. In addition, there are some cases in which GEF activity is dependent upon the presence of additional proteins [60], which could also be included in these assays.

This assay can be translated for use in high-throughput screening assays for small molecule regulators. The discovery of positive or negative regulators may prove useful to probe the physiological functions of GEFs and as possible leads for the development of drugs to treat diseases that are influenced by GEF mutations.

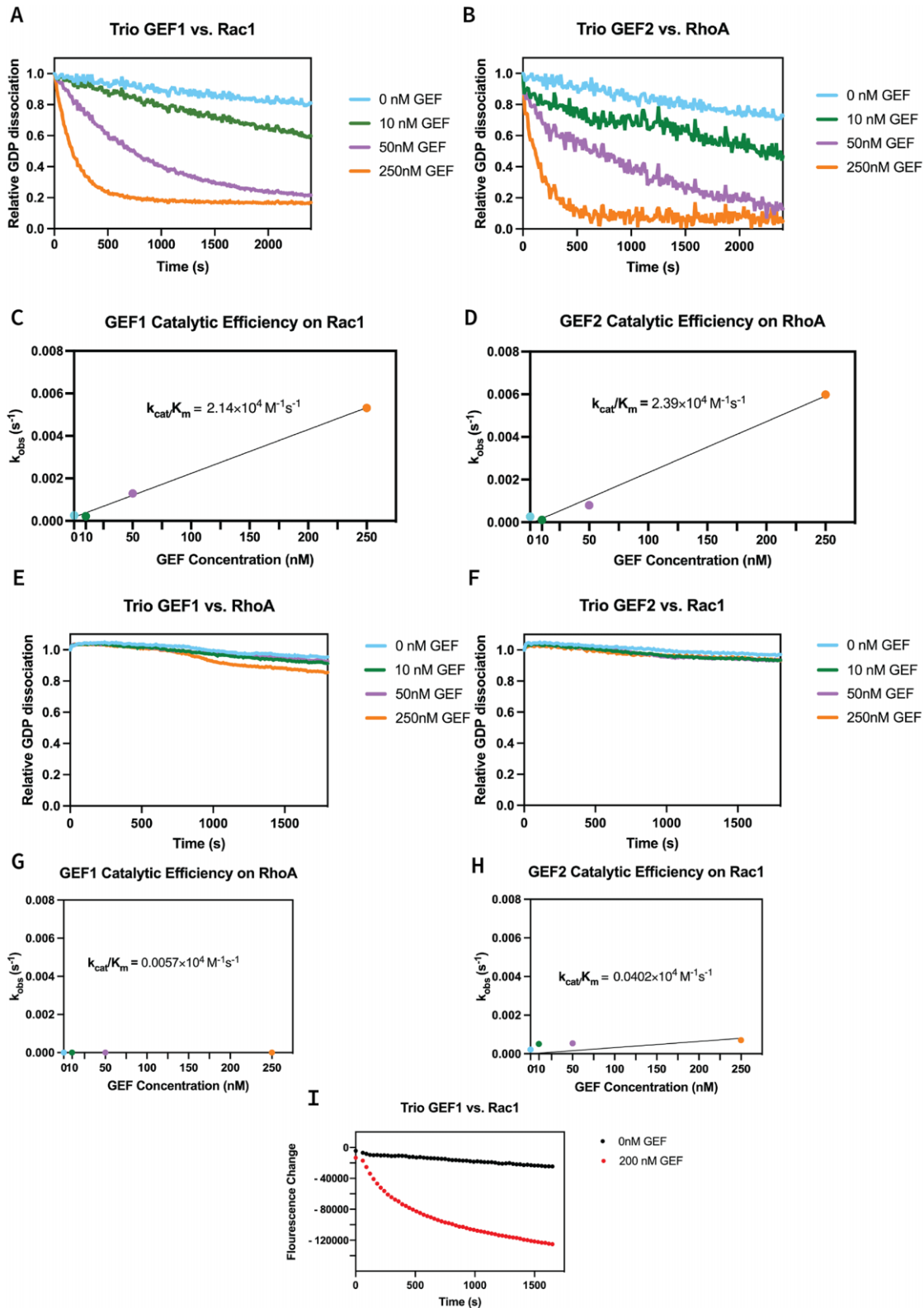


Figure 6: Fluorescence-based, GEF assay. Fluorescent GDP was incubated with the (A, E) Trio GEF1 (B, F) or Trio GEF2 domain at a specific concentration for 1 h. GEF activity was monitored by the decrease in fluorescence in a 96-well plate as GEF1 catalyzes the exchange of GDP for GTP on (A) Rac1 (E) and RhoA and as GEF2 catalyzes GDP-GTP exchange on (B) RhoA and Rac1 (F). Linear fit of initial rates plotted against (C, G) GEF1 (D, H) or GEF2 concentration. Linear fit of initial velocities yielded a k_{cat}/K_m of (C) $2.14 \times 10^4 \text{ M}^{-1} \text{ s}^{-1}$ for GEF1 on Rac1, (D) $2.39 \times 10^4 \text{ M}^{-1} \text{ s}^{-1}$ for GEF2 on RhoA, (G) $0.0057 \times 10^4 \text{ M}^{-1} \text{ s}^{-1}$ for GEF1 on RhoA, and (H) $0.0402 \times 10^4 \text{ M}^{-1} \text{ s}^{-1}$ for GEF2 on Rac1. (I) Single well readings for 384-well high-throughput screening assay of Trio GEF1 activity on Rac1. GEF1 was introduced into solution with BODIPY-FL-GDP and Rac1 in addition to small molecule regulators. The catalysis of GEF1 for the exchange of GTP for GDP on Rac1 is inhibited or promoted based on the small molecule regulators. The addition of GEF1 in a solution of Rac1 and BODIPY-FL-GDP catalyzes the exchange of GTP for GDP.

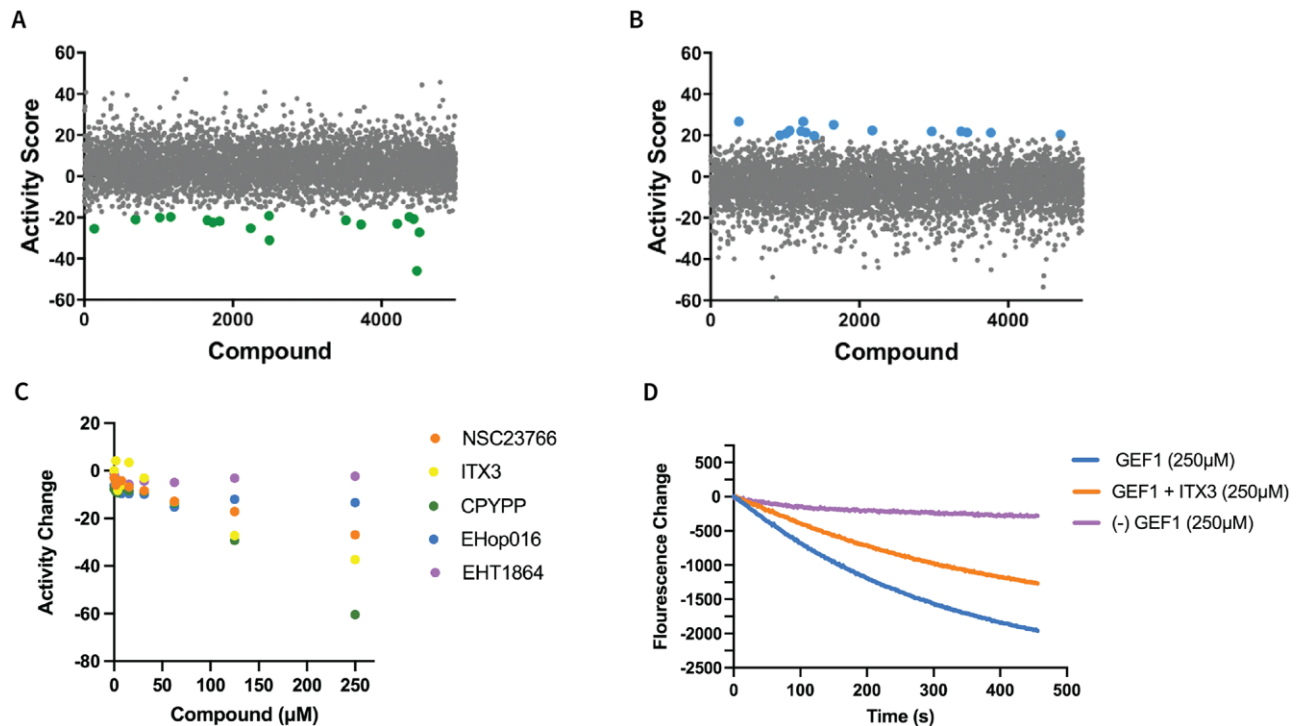


Figure 7: Trio GEF1 pilot screen results. 5100 compounds were screened at 30 μM in the Trio GEF1 FLIPR assay. Activity ratio score was calculated as a ratio of the compound condition versus the control condition. (A) Green dots represent the inhibitor hits. (B) Blue dots represent the activator hits and were calculated as compounds with an activity score of greater than three standard deviations from the mean of all compounds. (C) Trio GEF1 catalytic activity changes in the presence of known GEF1 inhibitors NSC23766, ITX3, CPYPP, EHOp016, and EHT1864. (D) Trio GEF1 catalytic activity in the presence of inhibitor ITX3.

Data availability

All the data presented are included in the article materials and further inquiries can be directed to the corresponding author.

Author contributions

A.M.B., E.E.C., and A.J.K. conceptualized and organized the project and wrote the manuscript. A.M.B., E.E.C., and A.J.K. performed cloning, protein purification, and GEF activity fluorescence assays. E.E.C. and A.M.B. performed the catalytic rate and efficiency calculations. E.S.W. generated code to process data. Y.-L.Z. optimized and performed high-throughput screening assay. J.R.C. supervised the high-throughput screen. A.J.K. supervised the entire project. All authors contributed to editing the manuscript.

Acknowledgements

We thank Josie Bircher and Daisy Duan for helpful comments on the manuscript.

Funding

This work was supported by the National Institute of Health (NIH) grants R56MH122449-01A1, R01 NS105640 and MH115939-04, and a SFARI Pilot Grant to A.J.K., R01 MH115939-04S1 to A.M.B., 1F31MH127891-01 to E.E.C., and the Stanley Center for Psychiatric Research to Y.-L.Z. and J.R.C.

Supplementary data

Supplementary data are available at *Biology Methods and Protocols* online.

Conflict of interest statement. The authors have no conflicts of interest to disclose.

References

- Etienne-Manneville S, Hall A. Rho GTPases in cell biology. *Nature* 2002;**420**:629–35.
- Ridley AJ, Hall A. The small GTP-binding protein rho regulates the assembly of focal adhesions and actin stress fibers in response to growth factors. *Cell* 1992;**70**:389–99.
- Ridley AJ, Paterson HF, Johnston CL et al. The small GTP-binding protein rac regulates growth factor-induced membrane ruffling. *Cell* 1992;**70**:401–10.
- Narumiya S, Tanji M, Ishizaki T. Rho signaling, ROCK and mDia1, in transformation, metastasis and invasion. *Cancer Metastasis Rev* 2009;**28**:65–76.
- Maekawa M, Ishizaki T, Boku S et al. Signaling from Rho to the actin cytoskeleton through protein kinases ROCK and LIM-kinase. *Science* 1999;**285**:895–8.
- Rohatgi R, Ma L, Miki H et al. The interaction between N-WASP and the Arp2/3 complex links Cdc42-dependent signals to actin assembly. *Cell* 1999;**97**:221–31.
- Takenawa T, Miki H. WASP and WAVE family proteins: key molecules for rapid rearrangement of cortical actin filaments and cell movement. *J Cell Sci* 2001;**114**:1801–9.
- Chen Z, Borek D, Padrick SB et al. Structure and control of the actin regulatory WAVE complex. *Nature* 2010;**468**:533–8.
- Spiering D, Hodgson L. Dynamics of the Rho-family small GTPases in actin regulation and motility. *Cell Adh Migr* 2011;**5**:170–80.
- Small JV, Stradal T, Vignall E et al. The lamellipodium: where motility begins. *Trends Cell Biol* 2002;**12**:112–20.

11. Condeelis J. How is actin polymerization nucleated in vivo? *Trends Cell Biol* 2001;11:288–93.
12. Bishop AL, Hall A. Rho GTPases and their effector proteins. *Biochem J* 2000;348:241–55.
13. Hart MJ, Eva A, Zangrilli D et al. Cellular transformation and guanine nucleotide exchange activity are catalyzed by a common domain on the dbl oncogene product. *J Biol Chem* 1994; 269:62–5.
14. Cherfils J, Chardin P. GEFs: structural basis for their activation of small GTP-binding proteins. *Trends Biochem Sci* 1999;24: 306–11.
15. Nomanbhoy TK, Cerione R. Characterization of the interaction between RhoGDI and Cdc42Hs using fluorescence spectroscopy. *J Biol Chem* 1996;271:10004–9.
16. Zohn IM, Campbell SL, Khosravi-Far R et al. Rho family proteins and Ras transformation: the RHOad less traveled gets congested. *Oncogene* 1998;17:1415–38.
17. Zheng Y, Fischer DJ, Santos MF et al. The faciogenital dysplasia gene product FGD1 functions as a Cdc42Hs-specific guanine-nucleotide exchange factor. *J Biol Chem* 1996;271: 33169–72.
18. Jian X, Gruschus JM, Sztul E et al. The pleckstrin homology (PH) domain of the Arf exchange factor Brag2 is an allosteric binding site. *J Biol Chem* 2012;287:24273–83.
19. Nawrotek A, Benabdi S, Niyomchon S et al. PH-domain-binding inhibitors of nucleotide exchange factor BRAG2 disrupt Arf GTPase signaling. *Nat Chem Biol* 2019;15:358–66.
20. Jezyk MR, Snyder JT, Gershberg S et al. Crystal structure of Rac1 bound to its effector phospholipase C-beta2. *Nat Struct Mol Biol* 2006;13:1135–40.
21. Chhatriwala MK, Betts L, Worthylake DK et al. The DH and PH domains of Trio coordinately engage Rho GTPases for their efficient activation. *J Mol Biol* 2007;368:1307–20.
22. Lee DM, Rodrigues FF, Yu CG et al. PH domain-Arf G protein interactions localize the Arf-GEF Steppke for cleavage furrow regulation in *Drosophila*. *PLoS ONE* 2015;10:e0142562.
23. Reckel S, Gehin C, Tardivon D et al. Structural and functional dissection of the DH and PH domains of oncogenic Bcr-Abl tyrosine kinase. *Nat Commun* 2017;8:2101.
24. Govek EE, Newey SE, Van Aelst L. The role of the Rho GTPases in neuronal development. *Genes Dev* 2005;19:1–49.
25. Shamah SM, Lin MZ, Goldberg JL et al. EphA receptors regulate growth cone dynamics through the novel guanine nucleotide exchange factor ephexin. *Cell* 2001;105:233–44.
26. Matsuo N, Hoshino M, Yoshizawa M et al. Characterization of STEF, a guanine nucleotide exchange factor for Rac1, required for neurite growth. *J Biol Chem* 2002;277:2860–8.
27. Yoshizawa M, Sone M, Matsuo N et al. Dynamic and coordinated expression profile of dbl-family guanine nucleotide exchange factors in the developing mouse brain. *Gene Expr Patterns* 2003;3:375–81.
28. Jaffe AB, Hall A. Rho GTPases: biochemistry and biology. *Annu Rev Cell Dev Biol* 2005;21:247–69.
29. Bircher JE, Koleske AJ. Trio family proteins as regulators of cell migration and morphogenesis in development and disease—mechanisms and cellular contexts. *J Cell Sci* 2021;134: jcs248393.
30. Miller MB, Yan Y, Eipper BA et al. Neuronal Rho GEFs in synaptic physiology and behavior. *Neuroscientist* 2013;19:255–73.
31. Watabe-Uchida M, Govek EE, Van Aelst L. Regulators of Rho GTPases in neuronal development. *J Neurosci* 2006;26: 10633–5.
32. Kutsche K, Yntema H, Brandt A et al. Mutations in ARHGEF6, encoding a guanine nucleotide exchange factor for Rho GTPases, in patients with X-linked mental retardation. *Nat Genet* 2000;26:247–50.
33. Marco EJ, Abidi FE, Bristow J et al. ARHGEF9 disruption in a female patient is associated with X linked mental retardation and sensory hyperarousal. *J Med Genet* 2008;45:100–5.
34. Pengelly RJ, Greville-Heygate S, Schmidt S et al.; DDD Study. Mutations specific to the Rac-GEF domain of TRIO cause intellectual disability and microcephaly. *J Med Genet* 2016;53: 735–42.
35. Machado CO, Griesi-Oliveira K, Rosenberg C et al. Collybistin binds and inhibits mTORC1 signaling: a potential novel mechanism contributing to intellectual disability and autism. *Eur J Hum Genet* 2016;24:59–65.
36. Papadopoulos T, Schemm R, Grubmuller H et al. Lipid binding defects and perturbed synaptogenic activity of a Collybistin R290H mutant that causes epilepsy and intellectual disability. *J Biol Chem* 2015;290:8256–70.
37. Katrancha SM, Wu Y, Zhu M et al. Neurodevelopmental disease-associated de novo mutations and rare sequence variants affect TRIO GDP/GTP exchange factor activity. *Hum Mol Genet* 2017;26:4728–40.
38. Ba W, Yan Y, Reijnders MR et al. TRIO loss of function is associated with mild intellectual disability and affects dendritic branching and synapse function. *Hum Mol Genet* 2016;25: 892–902.
39. Fromer M, Pocklington AJ, Kavanagh DH et al. De novo mutations in schizophrenia implicate synaptic networks. *Nature* 2014;506:179–84.
40. Girard SL, Gauthier J, Noreau A et al. Increased exonic de novo mutation rate in individuals with schizophrenia. *Nat Genet* 2011;43:860–3.
41. McCarthy SE, Gillis J, Kramer M et al. De novo mutations in schizophrenia implicate chromatin remodeling and support a genetic overlap with autism and intellectual disability. *Mol Psychiatry* 2014;19:652–8.
42. Sanders SJ, Murtha MT, Gupta A et al. De novo mutations revealed by whole-exome sequencing are strongly associated with autism. *Nature* 2012;485:237–41.
43. Debant A, Serra-Pages C, Seipel K et al. The multidomain protein Trio binds the LAR transmembrane tyrosine phosphatase, contains a protein kinase domain, and has separate rac-specific and rho-specific guanine nucleotide exchange factor domains. *Proc Natl Acad Sci USA* 1996;93: 5466–71.
44. Barbosa S, Greville-Heygate S, Bonnet M et al.; C4RCD Research Group. Opposite modulation of RAC1 by mutations in TRIO is associated with distinct, domain-specific neurodevelopmental disorders. *Am J Hum Genet* 2020;106: 338–55.
45. Ren XD, Schwartz MA. Determination of GTP loading on Rho. *Methods Enzymol* 2000;325:264–72.
46. Benard V, Bohl BP, Bokoch GM. Characterization of rac and cdc42 activation in chemoattractant-stimulated human neutrophils using a novel assay for active GTPases. *J Biol Chem* 1999;274:13198–204.
47. Moore KJ, Webb MR, Eccleston JF. Mechanism of GTP hydrolysis by p21N-ras catalyzed by GAP: Studies with a fluorescent GTP analogue. *Biochemistry* 1993;32:7451–9.
48. Leonard DA, Evans T, Hart M et al. Investigation of the GTP-binding/GTPase cycle of Cdc42Hs using fluorescence spectroscopy. *Biochemistry* 1994;33:12323–8.
49. Hong L, Kenney SR, Phillips GK et al. Characterization of a Cdc42 protein inhibitor and its use as a molecular probe. *J Biol Chem* 2013;288:8531–43.

50. Evelyn CR, Duan X, Biesiada J et al. Rational design of small molecule inhibitors targeting the Ras GEF, SOS1. *Chem Biol* 2014;**21**:1618–28.
51. Evelyn CR, Ferng T, Rojas RJ et al. High-throughput screening for small-molecule inhibitors of LARG-stimulated RhoA nucleotide binding via a novel fluorescence polarization assay. *J Biomol Screen* 2009;**14**:161–72.
52. Aittaleb M, Gao G, Evelyn CR et al. A conserved hydrophobic surface of the LARG pleckstrin homology domain is critical for RhoA activation in cells. *Cell Signal* 2009;**21**:1569–78.
53. Gao Y, Dickerson JB, Guo F et al. Rational design and characterization of a Rac GTPase-specific small molecule inhibitor. *Proc Natl Acad Sci USA* 2004;**101**:7618–23.
54. Zeinieh M, Salehi A, Rajkumar V et al. p75NTR-dependent Rac1 activation requires receptor cleavage and activation of an NRAGE and NEDD9 signaling cascade. *J Cell Sci* 2015;**128**:447–59.
55. Bouquier N, Vignal E, Charrasse S et al. A cell active chemical GEF inhibitor selectively targets the Trio/RhoG/Rac1 signaling pathway. *Chem Biol* 2009;**16**:657–66.
56. Nishikimi A, Uruno T, Duan X et al. Blockade of inflammatory responses by a small-molecule inhibitor of the Rac activator DOCK2. *Chem Biol* 2012;**19**:488–97.
57. Montalvo-Ortiz BL, Castillo-Pichardo L, Hernández E et al. Characterization of EHOp-016, novel small molecule inhibitor of Rac GTPase. *J Biol Chem* 2012;**287**:13228–38.
58. Shutes A, Onesto C, Picard V et al. Specificity and mechanism of action of EHT 1864, a novel small molecule inhibitor of Rac family small GTPases. *J Biol Chem* 2007;**282**:35666–78.
59. Sadybekov A, Tian C, Arnesano C et al. An autism spectrum disorder-related de novo mutation hotspot discovered in the GEF1 domain of Trio. *Nat Commun* 2017;**8**:601.
60. Wilkinson B, Li J, Coba MP. Synaptic GAP and GEF complexes cluster proteins essential for GTP signaling. *Sci Rep* 2017;**7**:5272.